Ionization of molecules by multicharged bared ions by using the stoichiometric model

author

Instituto de Astronomía y Física del Espacio
(CONICET-UBA). Casilla de correo 67, sucursal 28
(C1428EGA) Buenos Aires, Argentina.

September 19, 2019

Abstract

1 Introduction

The damage caused by the impact of multicharged heavy projectiles has become a field of interest due to its recent implementation in ion-beam cancer therapy. The effectiveness of the radiation depends on the choice of the ions. In particular, theoretical and experimental studies with different projectiles have concluded that charged carbon ions could be the most suitable ions to use. The study of such systems represent a challenge from the theoretical point of view. The most widely used method to compute ionization of multicharged atoms is the first Born approximation. This perturbative method warrants the Z^2 laws, where Z is the projectile charge. However, the damage concentrated in the vicinities of the Bragg peak correspond to energies of hundreds of KeV/amu. Precisely in this region, often refered to as the intermediate energy region, the Born approximation starts to fail. Another theoretical issue arises from the targets themselves; we are dealing with complex molecules. This article deals precisely with these two aspects. First, we

perform more appropriate calculations on the primary damage mechanism, i.e., atomic ionization by multicharged ions, which can replace the Born results. Second, we inspect and use an stoichiometric model, which reduces a molecule to a sum of atomic processes quantities weighted by the number of such atom in the molecule.

To overcome the first perturbative approximation limitations, and since the projectiles are multicharged ions, we resort to the Continuum Distorted Wave-Eikonal Initial State (CDW), which includes higher perturbative corrections. We start from the premise that the ionization process is the mechanism that deposits the most significant amount of primary energy. This process produces an electron-energy spectrum that needs to be integrated. Moreover, the ejected electrons become a new source of local damage. These secondary electrons are included in Monte Carlo simulations and hence their behavior must be investigated. With this end in mind, we calculate not only the ionization cross-sections but also energy and mean angular distributions of the emitted electrons.

The molecular structure complexity of the target is dealt with by implementing the simplest stoichiometric model (SSM); we assume that the molecule is composed of isolated independent atoms. In all cases, the total cross-section is simply the sum of the cross-section of each atom.

Then, by implementing the SSM and the CDW –instead of the first Born approximation–, we calculate ionization cross-section of several molecules (see Table 1) by the impact of antiprotons, H^+, He^{+2}, Be^{+4}, C^{+6}, and O^{+8}. Furthermore, in Section 3, we investigate different DNA and RNA molecules such as adenine, cytosine, guanine, thymine, uracil, tetrahydrofuran (THF), pyrimidine and also DNA backbone.

The results are processed to test the Toburen scaling rule, which states that the ratio between the ionization cross-section and the number of valence electrons (outer electrons) in terms of the projectile velocity can be arranged in a narrow universal band. We have also applied this rule to several hydrocarbons and nucleobases. In Section 3.2, we will prove that the width of the resulting universal band can be significantly reduced if we redefine the effective number of valence electrons.

It is well known that the residual electrons from the ionization process cause significant biological damage. To inspect this mechanism, in Section 3.3 and 3.4, we calculated the mean electron energy and angular distributions. Surprisingly, we found a substantial dependence of the charged projectile, which is unexpected in the first Born approximation.

The hefty charge projectiles are dealt with the CDW. However, the stoichiometric model used seems to be very simplistic. The approximation considers each atom as neutral, which is not correct. In Section 3.5, we used the molecular electronic structure code GAMESS [1] to calculate the excess or defect of electron density one each atom. Then, the simple stoichiometric model is modified to account for the departure from neutrality of the atoms. We find that for the DNA molecules this modification does not introduce a substantial change.

2 Theory: Ionization of Atoms

In our study, we will consider six atoms α = H, C, N, O, P, and S. Most of the organic molecules are composed of these atoms. Some particular molecules also include halogen atoms such as fluor and bromine; ionization cross-sections of these elements have been previously published [2, 3].

The total ionization cross-sections of these atoms were calculated using the CDW. The initial bound and final continuum radial wave functions were obtained by using the RADIALF code, developed by Salvat and coworkers, and a Hartree-Fock potential obtained from the Depurated Inversion Model [4, 5]. We used a few thousand pivot points to solve the Schrödinger equation, depending on the number of oscillations of the continuum state. The radial integration was performed using the cubic spline technique. The number of angular momenta considered varied from 8, at very low ejected-electron energies, up to 30, for the highest energies considered. The same number of azimuth angles were required to obtain the four-fold differential cross-section. The calculation performed does not display prior-post discrepancies at all. Each atomic total cross-section in Eq. (1) was calculated using 35 to 100 momentum transfer values, 28 fixed electron angles, and around 45 electron energies depending on the projectile impact energy. Further details of the calculation are given in Ref. [6]. Simultaneously, we will be reporting state to state ionization cross sections for these cases in Ref. [7], which will be very useful to estimate molecule fragmentation.

In Fig. 1, we report our total ionization results for the six essential elements by the impact of six different projectiles: antiprotons, H^+, He^{+2}, Be^{+4}, C^{+6}, and O^{+8}. To reduce the resulting 36 magnitudes into a single consistent figure, we considered the fact that in the first Born approximation the ionization cross-section scales with the square of the projectile charge,

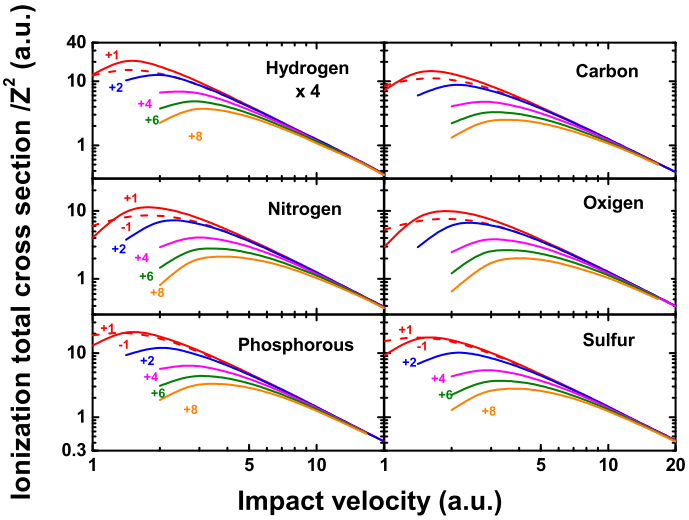

Figure 1: Scaled total ionization cross section of six atomic targets by impact of multicharged projectiles.

Z^2. The values of the impact energies considered range between 0.1 to 10 MeV/amu, where the CDW is supposed to hold. In fact, for the highest projectile charges the minimum impact energy where the CDW is expected to be valid could be higher than 100 KeV. Moreover, we corroborated that the first Born approximation provides quite reliable results only for energies higher than a couple of MeV/amu. We use the same color to indicate the projectile charge throughout the figures of this work: dashed-red, solid-red, blue, magenta, olive and orange for antiprotons, H^+, He^{+2}, Be^{+4}, C^{+6}, and O^{+8}, respectively. The charge state of the projectiles are also given in the figures. Notably, there is no complete tabulation of ionization of atoms by the impact of multicharged ions. We hope that the ones presented in this article will be of help for future works.

3 Ionization of Molecules

3.1 The stoichiometric model

Lets us consider a molecule M composed by n_α atoms of the element α, the SSM describes the total ionization cross section of the molecule σ_M as a

simple sum of ionization cross sections of the isolated atoms σ_α,

$$\sigma_M = \sum_\alpha n_\alpha \sigma_\alpha \,. \tag{1}$$

We divided sixteen molecular targets of our interest in three families. The classification defined is given in Table 1.

CH	CH_4 (methane), C_2H_2 (acetylene), C_2H_4 (ethene), C_2H_6 (ethane), C_6H_6 (benzene)
CHN	C_5H_5N (pyridine), $C_4H_4N_2$ (pyrimidine), C_2H_7N (dimenthylamine), CH_5N (monomethylamine)
DNA	$C_5H_5N_5$ (adenine), $C_4H_5N_3O$ (cytosine), $C_5H_5N_5O$ (guanine), $C_5H_6N_2O_2$ (thymine), $C_4H_4N_2O_2$ (uracil), C_4H_8O (THF), $C_5H_{10}O_5P$ (DNA backbone), $C_{20}H_{27}N_7O_{13}P_2$ (dry DNA)

Table 1: Molecular targets of our interest classified in three families.

We report the total ionization cross sections by the impact of multicharged ions for adenine, cytosine, guanine and thymine in Fig. 2. For adenine, the agreement with the experimental data available [8] is very good in our range of validity. To the best of our knowledge, there are not experimental data on ion–collision ionization for the rest of the molecules. We included electron impact measurements [9] with the corresponding equivelocity conversion for incident energies higher than 500 keV. In this region, the proton and electron cross section should agree. Although the electron impact measurements are above our findings for all the molecular targets, it is worth stating that our results agree very well with other theoretical predictions [10, 11].

Our calculations for uracil, DNA backbone, pyrimidine and THF are given in Fig. 3. For uracil, we have good agreement with the experimental proton impact measurements by Itoh *et al.* [12]. However, for the same target, our theory fails by a factor of two for the experimental ionization values by the impact of C^{+4}, O^{+6} and O^{+8} ions [13, 14]. Nonetheless, it should be stated that our theoretical results coincide with calculations by Champion, Rivarola and collaborators [13, 15], which may indicate a possible misstep of the experiments. For pyrimidine, we show comparison of our results with experimental data for proton [16] and electron [17] ionization. The electron impact

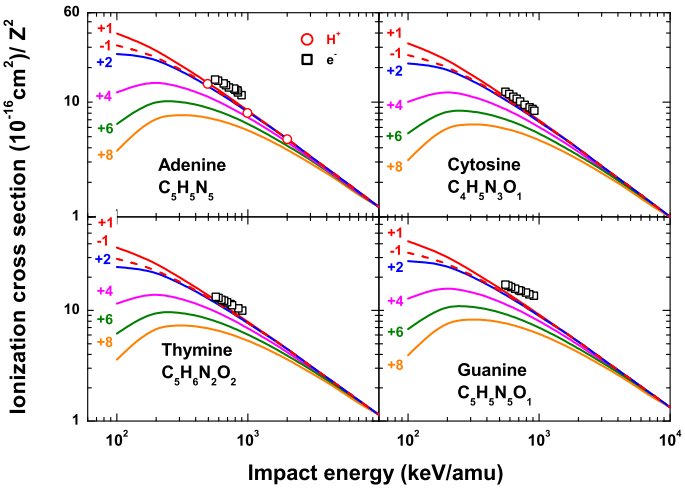

Figure 2: Scaled ionization cross section by impact of multicharged ions. Experiments: ∘ [8] for proton impact and □ [9] for electron impact with equivelocity conversion.

measurements agree with our calculations for energies higher than 500keV. Unexpectedly, the proton impact cross sections are significantly lower than our findings. The THF molecule results are compared with proton [18] and electron [17, 19, 20] impact measurements, showing overall good agreement with our theory.

3.2 Scaling rule

3.2.1 Toburen numbers

The first attempt to develop a comprehensive but straightforward phenomenological model for electron ejection from large molecules was proposed by Toburen *et al.* [24, 25]. The authors found it convenient to scale the experimental ionization cross section in terms of the number of active or weakly–bound valence electrons n_e (i.e. total number of electrons minus the K–shell). Following Toburen, we can define the ionization cross section per weakly bound

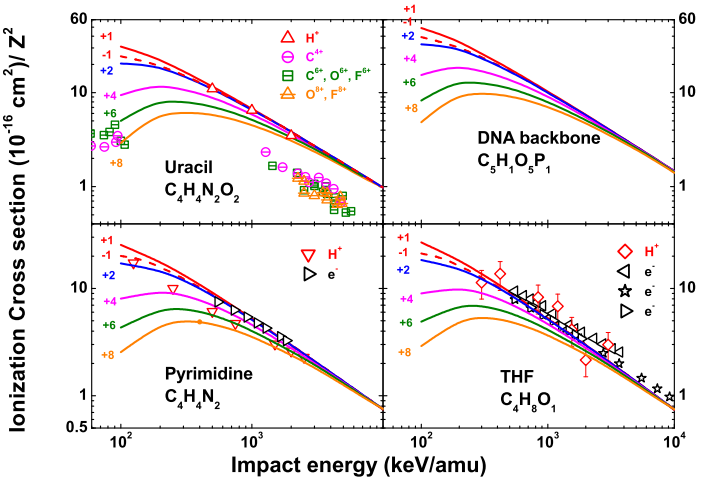

Figure 3: Scaled ionization cross section by impact of multicharged ions. Experiments: proton impact on △ uracil [12], ▽ pyrimidine [16] and ◇ THF [18]. Impact of ⊖ C^{+4}, ⊟ C^{+6}, O^{+6}, F^{+6}, and ⧋ O^{+8}, F^{+8} on uracil [13, 14]. Symbols ▷ [17], ◁ [19], and ☆ [20] for electron impact with equivelocity conversion.

electron, σ_e^T, as

$$\sigma_e^T = \frac{\sigma_M}{n_e} = \frac{\sum\limits_\alpha n_\alpha \sigma_\alpha}{\sum\limits_\alpha n_\alpha \nu_\alpha^T} = \sigma_e^T(v)\,, \tag{2}$$

where ν_α^T are the Toburen numbers for each α atom is given by

$$\nu_\alpha^T = \begin{cases} 1, & \text{for H,} \\ 4, & \text{for C,} \\ 5, & \text{for N and P,} \\ 6, & \text{for O and S.} \end{cases} \tag{3}$$

The Toburen rule can be stated by saying that σ_e is a *universal* parameter independent on the molecule, which depends solely on the impact velocity, and holds for high impact energies (i.e. 0.25–5 Mev/amu). These ν_α^T can be interpreted as the number of active electrons in the collision. Of course, at very high energies also de K–shell electrons will be ionized and these numbers will be different. A similar dependence with the number of weakly bound electrons was found in Ref. [12] for proton impact on uracil and adenine.

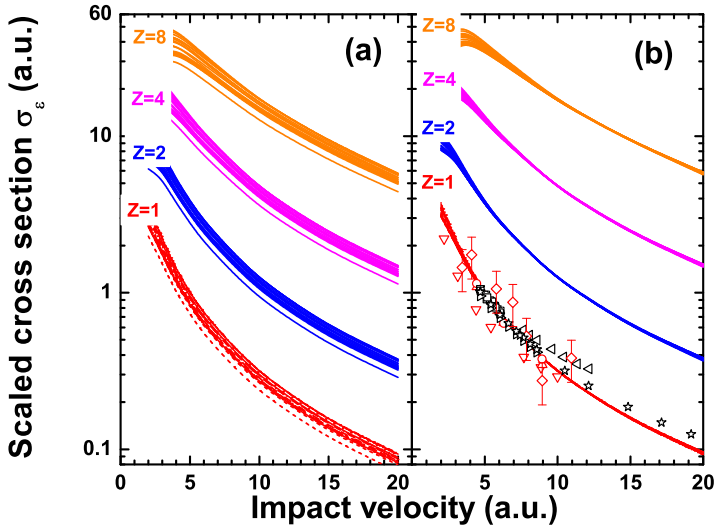

Figure 4: Scaled ionization cross section per weakly bound electron using (a) the Toburen numbers ν_α^T, and (b) our proposed numbers $\nu_\alpha^{\rm CDW}$. Experiments: proton impact on $\circ$ adenine [8], $\triangle$ uracil [12], $\triangledown$ pyrimidine [16] and $\diamond$ THF [18]; electron impact on $\triangleright$ pyrimidine [17], and $\triangleleft$, $\star$ [19, 20] THF.

Our CDW results for σ_e^T are shown in Fig. 4a as a function of the impact energy for different projectile charges computed with the SSM for the molecular targets from Table 1. The universality with Z is the one provided by Born approximation, i.e., $\sigma_e^T(Z) = Z^2\sigma_e^T(Z=1)$, and it holds for large impact velocities, as shown Fig. 4a. Of course, for lower impact velocities, the CDW breaks the behavior of the Z^2 rule. Although the Toburen scaling holds for high energies, its performance is still not satisfactory: the universal band is quite broad.

3.2.2 New scaling

The departure of our theoretical results from the Toburen rule can be easily understood by inspecting Fig. 1. It can be noted that the rule $\sigma_\alpha/\nu_\alpha^T \sim \sigma_e^T$, approximatelly constant, is not well satisfied by the CDW. For example, Fig. 1 shows that the cross sections for O are actually very similar to the cross sections for C, suggesting 4 active electrons in O instead of 6. In the

same way, the number of active electrons for N, P and S are also different from the ν_α^T of Eq. (3).

Based on the CDW results, we propose a new scaling,

$$\sigma_e = \frac{\sigma_M}{\sum\limits_\alpha n_\alpha \nu_\alpha^{\rm CDW}}, \tag{4}$$

where σ_M follows Eq. (1), and $\nu_\alpha^{\rm CDW}$ are the new active–electron numbers per atom obtained from the CDW ionization cross sections for different ions in H, C, N, O, P , and S targets. Our proposed active–electron numbers are

$$\nu_\alpha^{\rm CDW} \sim \begin{cases} 1, & \text{for H,} \\ 4, & \text{for C, N, and O,} \\ 4.5, & \text{for P and S.} \end{cases} \tag{5}$$

The new scaled cross sections σ_e are plotted in Figure 4b. A much better sharp band is observed, especially for impact energies $E = (0.5-8)$ MeV/amu for $Z = 1$ and $Z = 2$, and $E = (2.5-8)$ MeV/amu for $Z > 2$. In fact, the experimental data for ionization of adenine [8], uracil [12], pyrimidine [16] and THF [18] by proton impact seems to corroborate the new scaling. We also included the electron impact ionization measurements with equivelocity conversion on pyrimidine [17], and THF [17, 19, 20]. It will be interesting to cross–check for experiments with higher projectile charge states.

Molecule	n_e	Molecule	n_e	Molecule	n_e
H_2	2	C_2H_7N	19	$C_4H_5N_3O$	37
H_2O	6	C_4H_8O	28	$C_5H_6N_2O_2$	42
NH_3	7	$C_4H_4N_2$	28	$C_5H_5N_5$	45
CH_4	8	C_6H_6	30	$C_5H_5N_5O$	49
CH_5N	13	$C_4H_4N_2O_2$	36	$C_5H_{10}O_5P$	54.5

Table 2: New scaling numbers for some molecular targets of biological interest.

By using Eq. (5), the number of active electrons $n_e = \sum_\alpha n_\alpha \nu_\alpha^{\rm CDW}$ can be redefined. We give new values in Table 2 for some molecules of interest. These values are very different from the ones proposed by Toburen and used by other authors [12]. Moreover, an alternative way of showing the scaling

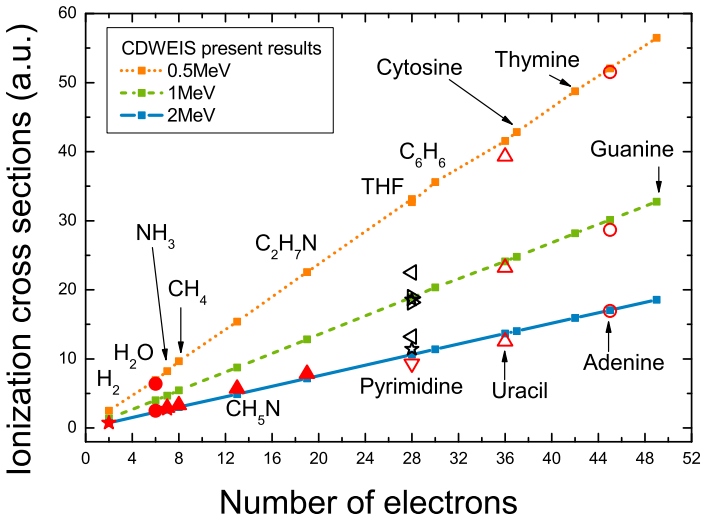

Figure 5: Ionization cross sections by impact of protons at 0.5, 1 and 2 MeV in terms of the number of active electrons given by Table 2. Experiments: ∘ adenine [8], △ uracil [12], ▽ pyrimidine [16], ▲ $C2H_7N$, CH_5N, methane and amonia [21], ★ amonia and H_2 [22], and • water [23].

can be attained by plotting the ionization cross sections of molecules as a function of the number of active electrons from Table 2. Our findings are displayed in Fig. 5 for impact energies 0.5, 1 and 2 MeV. As can be noted, the computed CDW ionization cross sections for all the molecules show a linear dependence with the number of electrons from Table 2. We obtain similar results even for $E = 10$ MeV. The comparison with the experimental data available shows very nice agreement, from the smallest molecules, H_2, H_2O and CH_4, up to the most complex ones, like adenine or guanine. In some cases, the experimental data were interpolated. Care was taken in such procedure.

3.3 Emitted electron energies

In a given biological medium, direct ionization by ion impact accounts for just a fraction of the overall damage. Secondary electrons, as well as recoil target ions, also contribute substantially to the total damage. We can consider

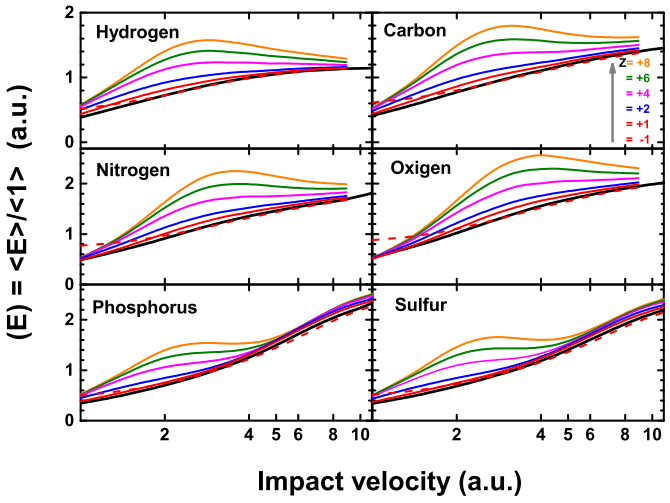

Figure 6: Mean emitted energy distribution for ionization by impact of multicharged ions.

the single differential cross section of the shell nl of the atom α, $d\sigma_{\alpha nl}/dE$, to be a function of the ejected electron energy E as a simple distribution function [26]. Then, we can define the mean value $\overline{E}_\alpha$ as in Ref. [27],

$$\overline{E}_\alpha = \frac{\langle E_\alpha \rangle}{\langle 1 \rangle} = \frac{1}{\sigma_\alpha} \sum_{nl} \int dE\, E \frac{d\sigma_{\alpha,nl}}{dE}\,, \tag{6}$$

$$\langle 1 \rangle = \sigma_\alpha = \sum_{nl} \int dE\, \frac{d\sigma_{\alpha,nl}}{dE}\,, \tag{7}$$

where Σ_{nl} takes into account the sum of the different sub-shell contributions of the element α.

Figure 6 shows $\overline{E}_\alpha$ for six elements from Table 1. The range of impact velocities was shorten up to v = 10 a.u. due to numerical limitations in the spherical harmonics expansion. In our theoretical treatment, we expand our final continuum wave function as per usual,

$$\psi^-_{\vec{k}}(\vec{r}) = \sum_{l=0}^{l_{\max}} \sum_{m=-l}^{l} R^-_{kl}(r) Y_l^m(\widehat{r}) Y_l^{m^*}(\widehat{k})\,. \tag{8}$$

We are confident with our calculations up to $l_{\max} \sim 30$. As the impact velocity v increases, so do $\langle E_\alpha \rangle$ and $l_{\max}$, which results in the inclusion of very oscilla-

tory functions in the integrand. Furthermore, the integrand of $\langle E_\alpha \rangle$ includes the kinetic energy E (see Eq. (6)), which cancels the small energy region and reinforces the large values, making the result more sensible to large angular momenta. Regardless, for $v > 10$ a.u., the first Born approximation holds.

In Figure 6 , we estimate $\overline{E}_\alpha$ in the 0.5–2 a.u. velocity range, or equivalently from 15 to 50 eV, for all the targets. Our results agree with the experimental findings [26]. The dependence of the mean energy value with the projectile charge Z is surprisingly sensible, which can duplicate the proton results. This effect can be attributed to the depletion caused by the multicharged ions to the yields of low energy electrons. In the high approximation, surviving the Z^2 law. Then, the ratio in Eq. (6) cancels out and $\overline{E}_\alpha$ becomes a universal value independent on Z.

Extending the simple stoichiometric model for the mean electron energy calculation, it results

$$\overline{E}_M = \frac{\sum\limits_\alpha n_\alpha \overline{E_\alpha}}{\sum\limits_\alpha n_\alpha \sigma_\alpha}. \tag{9}$$

For impact of H^+ and He^{+2} on water at 1 MeV/amu, we obtain $\overline{E}_{H_2O} = 43.7$ and 45 eV, while the experimental values on liquid water by Pimblott and LaVerne [32] were found to be 51.5 and 52.2 eV, respectively. Just to stress the importance of the projectile charge, for O^{+8} on water, at the same impact energy 1 MeV/amu, we obtained $\overline{E}_{H_2O} = 54.7$ eV, which is 25% larger than proton impact result. It is worth noting that there should not be any difference if the calculations were carried in first Born approximation. We will came back on this issue later.

3.4 Emitted electron angles

As mentioned before, secondary electrons contribute to the total damage. Then, not only is the ejection energy important but also the angle of emission. Once again, we can consider the single differential cross section in terms of the ejected electron solid angle Ω, $d\sigma_{\alpha,nl}/d\Omega$, to be expressed as a distribution function, and the mean angle $\overline{\theta}_\alpha$ can be defined as

$$\overline{\theta}_\alpha = \frac{\langle \theta_\alpha \rangle}{\langle 1 \rangle} = \frac{1}{\sigma_\alpha} \sum_{nl} \int d\Omega \, \theta \, \frac{d\sigma_{\alpha,nl}}{d\Omega} \tag{10}$$

Figure 7 shows $\overline{\theta}_\alpha$ for our six elements of interest. A new important dependence of $\overline{\theta}_\alpha$ with Z is observed. It is a general belief [33] that the angular

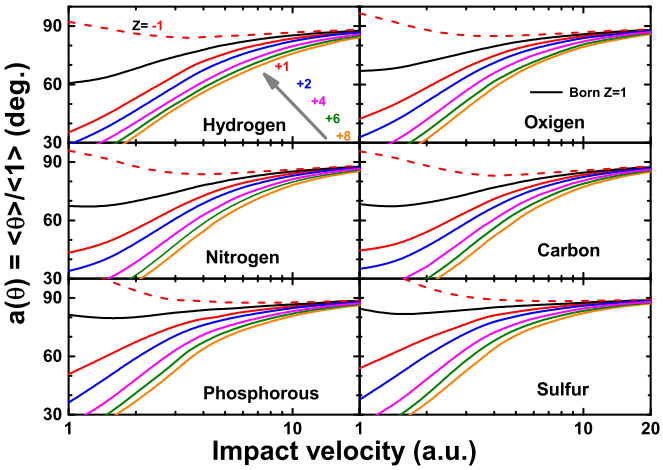

Figure 7: Mean emitted angle distribution for ionization by impact of multicharged ions.

dispersion of emitted electrons are nearly isotropic. This effect is caused by the insignificant angular anisotropy of sub-50-eV yield. A typical value for the ejection angle considered in the literature is $\overline{\theta}_\alpha \sim 70^\circ$ [26], and it is quite correct in the range of validity of the first Born approximation for any target. But, when a distorted wave approximation is used, $\overline{\theta}_\alpha$ decreases substantially with Z in the intermediate energy region, as observed in Figure 7. For example, for C^{+6} impact, the Bragg peak occurs at 0.3 MeV/amu, where $\overline{\theta}_\alpha$, computed with the CDW method, is about half of the value obtained with the first Born approximation. This correction should close the damage to the forward direction.

We can attribute this correction to the capture to the continuum effect; the larger the charge Z, the smaller $\overline{\theta}$ will be. Of course, this effect only holds at intermediate energies and not at high impact energies, where the Born approximation rules. One illustrative observation is the behavior of antiprotons: the projectile in this case repels the electrons, making the distribution almost symmetric. Note the opposite effect of proton and antiprotons; they run one opposite to the other, as compared with the first Born approximation.

3.5 A modified stoichiometric model

The SSM considers the molecule to be assembled by isolated neutral atoms, which is definitively unrealistic. A first improvement can be suggested by assuming that the atoms are not neutral and that they have an uneven distribution of electrons within the molecule; this distribution can be given by an effective charge q_α. A possible value for q_α is given by the Mulliken charge. However, there are a wide variety of charge distributions, such as the net or natural atomic charge [28], the Löwdin charge, etc.

Consider that the total amount of electrons Q_α on the element α are equally distributed on all the α atoms. Therefore, each element α will have an additional charge: $q_\alpha = Q_\alpha/n_\alpha$, which can be positive or negative. This value will depend on the relative electronegativity value with respect to the other atoms [29]. Now, instead of an integer number of elements n_α of the atom α, we have a fractional number of atoms given by

$$n'_\alpha = n_\alpha - \frac{q_\alpha}{\nu_\alpha^{\mathrm{CDW}}} \tag{11}$$

In the case of neutral atoms, $q_\alpha = 0$ and we recover $n'_\alpha = n_\alpha$, as it should be.

To inspect the effect of q_α, we computed the molecular structure of several nucleobases with the GAMESS code. We used the 6-31G(d,p) basis set, which includes polarization functions for all the atoms. The calculations were carried out implementing the B3LYP functional [30, 31] to account for the correlation and exchange effects. In Table 3, we display the charge q_α of four DNA molecules.

Element	C	H	N	O	New stoichiometry
Adenine	+0.32	+0.23	–0.55		$C_{4.92}H_{4.77}N_{5.14}$
Cytosine	+0.28	+0.21	–0.56	–0.53	$C_{3.93}H_{2.79}N_{5.14}O_{1.13}$
Guanine	+0.46	+0.20	–0.58	–0.36	$C_{4.89}H_{4.80}N_{5.15}O_{1.09}$
Thymine	+0.20	+0.19	–0.54	–0.52	$C_{4.95}H_{1.95}N_{6.13}O_{2.13}$

Table 3: Effective charge q_α and new stoichiometric formula defined by Eq. (11) for four DNA molecules.

The molecular binding energies of the outer electrons for adenine, cytosine, guanine and thymine are shown in Fig. 8. On the left side of the figure, we show the atomic Hartree–Fock energies of the constituent elements, which

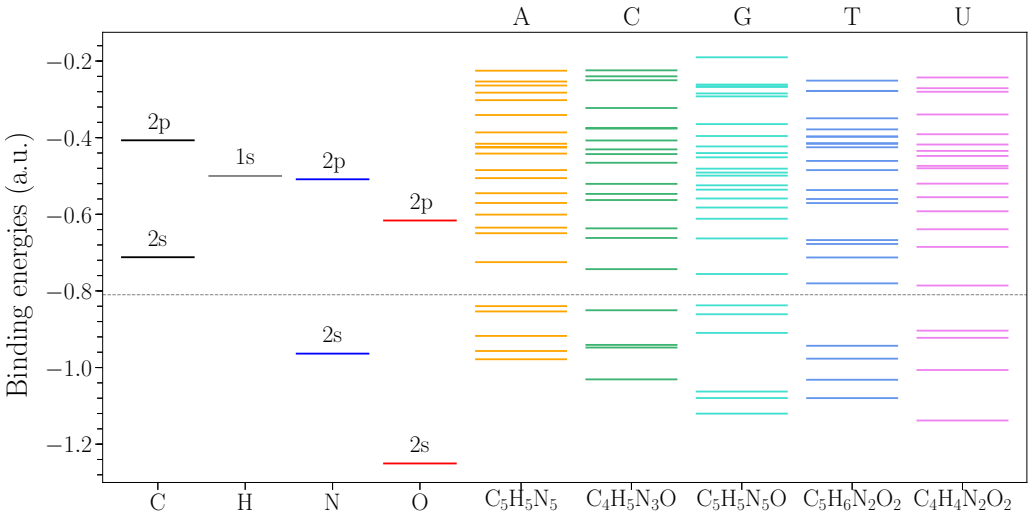

Figure 8: Theoretical molecular binding energies for adenine, cytosine, guanine, thymine and uracil compared to those of atomic constituents.

can give an idea of how the molecular levels distribute. A dashed line around −0.8 a.u. is drawn to separate in two the band levels of the outer electrons. The electrons in the molecular targets corresponding to the $2s$ of N and C in the atomic case are placed in a secondary gap. The lower levels of the secondary gap correspond to the oxygen. The number of electrons in the valence shell for all O would seem to be equal to 4, as previously setted by the scaling rule Eq. (5). The N case is not as straightfoward; the electrons that would correspond to the $2s$ are located just below the line. The $\nu_\alpha^{\mathrm{CDW}}$ value given for N would suggest that a significant amount of electron density from the secondary gap is shared with the valence band.

By implementing Eq. (11), it is possible to determine a new stoichiometric formula (last column of Table 3). Now, instead of having an integer number of atoms n_α, we obtain a fractional number n'_α. Molecular cross sections σ' can be computed considering such values. Relative errors for the ionization cross sections were computed for the DNA bases from Table 3. The differences obtained were of just very few percents, which indicates that the modified SSM is a quite robust model to handle these type of molecule within the range error expected for this model.

3.5.1 Ionization of water

Considering that the residual charge of each hydrogen in water is $q_{\mathrm{H}} = +0.35$ [29], we can imply that the residual charge of oxygen is $q_{\mathrm{O}} = -0.7$. Then, we could re-write the formula of water using Eq. (11) as $\mathrm{H}_{1.3}\mathrm{O}_{1.17}$ (assuming $n_{\mathrm{O}}^{\mathrm{CDW}} \simeq 4$ and $n_{\mathrm{H}}^{\mathrm{CDW}} \simeq 1$). Recalculating the mean electron energy by the impact of H^{+} and He^{+2} on water at 1 MeV/amu, we obtain $\overline{E}_{\mathrm{H_2O}} = 46.2$ and 47.6 eV. Our results are 10% apart from the experimental values: 51.5 and 52.2 eV [32], respectively, which is not bad considering the simplicity of our model.

We can be compute the fraction of energy carried by the electron f, which is defined as

$$f = \frac{\sum\limits_{\alpha} n_{\alpha}\sigma_{\alpha}\overline{E_{\alpha}}}{\sum\limits_{\alpha} n_{\alpha}(\sigma_{\alpha}\overline{E_{\alpha}} + \sum\limits_{nl}\sigma_{\alpha nl}E_{\alpha nl})}\,. \tag{12}$$

Using our shell-to-shell ionization cross sections $\sigma_{\alpha nl}$ [7], and the atomic binding energies $E_{\alpha nl}$ [34] of the atom α, we obtain $f = 0.70$ and 0.71 on water at 1 MeV/amu for H^{+} and He^{+2}, which differ from the respective experimental values $f = 0.81$ and 0.80.

The difference between our calculations and the experimental values could be attributed to the binding energy values of the molecular water 12.65 eV with respect to its atomic components, H (13.6 eV) and O (17.19 eV). This theoretical discrepancy goes beyond our independent atom approximation and it cannot be accounted for by our model. Once again, we could estimate this contribution by resorting to the stoichiometric model. We can make an assesment for a maximum difference per molecule of water as

$$\delta E = (13.6 - 12.65) \times 1.17 + (17.19 - 12.65) \times 1.3 = 7\,\mathrm{eV} \tag{13}$$

Most of this energy should be transfer to the kinetic energy of the emitted electron. Thus, by adding 7 eV to the previous values, we obtain $\overline{E}_{\mathrm{H_2O}} = 53.2$ and 54.6 eV for H^{+} and He^{+2} on water at 1 MeV/amu, respectively, which are much closer to the experimental values. If we add δE to the numerator of Eq. (12), we obtain $f = 0.81$ and 0.80, in perfect agreement with the experiments (see Table 1 of Ref. [32]).

4 Conclusions

We calculated ionization cross sections by impact of antiprotons, H^+, He^{+2}, Be^{+4}, C^{+6}, and O^{+8} for seventeen molecules containing H, C, N, O, P and S with the CDW method. The importance of the influence of Z was observed in the mean energy $\overline{E}_\alpha$ and angle $\overline{\theta}_\alpha$. For a given target α, as the nuclear charge of the projectile Z increases, so does the mean energy of emittion $\overline{E}_\alpha$. Conversely, the mean angle of emission $\overline{\theta}_\alpha$ decreases. At high impact energy, say larger than 1 MeV/amu, these values converge to the Born approximation, which embodies the simple Z^2 law. The seventeen molecules selected were investigated using the simple stoichiometric model. Results for eigth DNA bases were presented and compared with the sparse available experiments. We explore the rule of Toburen which scales all the molecular ionization cross section when divided by the number of weakly bound valence electrons ν_α^T given by Eq. (2). We found the rule scales much better when normalizing our theoretical ionization cross sections to the number $\nu_\alpha^{\rm CDW}$ given by Eq. (5). Finally, we attempt to improve the stoichiometric model by using the Mulliken charge to define a new model containing fractional rather than integer proportions. No substantial correction was found, which indicates that our modified SSM works quite well. By inspecting the molecular binding energy from quantum mechanical structure calculations, we were able to understand the values defined for $\nu_\alpha^{\rm CDW}$.

The main objective of this article is to provide the tools to estimate any inelastic parameter parameter –such as emission angle, emitted mean energy and cross section– by the impact of any multicharged on any molecule containing H, C, N, O, P and S, with the help of the stoichimetrical model. Our goal was quite ambitious, considering the simplicity of our proposal. However, we think our results could be used to estimate the ionization magnitude with an acceptable level of uncertainty.

References

[1] M. W. Schmidt, K. K. Baldridge, J. A. Boatz, S. T. Elbert, M. S. Gordon, J. H. Jensen, S. Koseki, N. Matsunaga, K. A. Nguyen, S. J. Su, T. L. Windus, M. Dupuis, J. A. Montgomery J. Comput. Chem. 14, 1347-1363 (1993)

[2] J. E. Miraglia and M. S. Gravielle. Ionization of the He, Ne, Ar, Kr, and Xe isoelectronic series by proton impact. Phys Rev A **78**, 052705 (2008)

[3] J. E. Miraglia, Ionization of He, Ne, Ar, Kr, and Xe by proton impact: Single differential distributions. Phys. Rev. A **79**, 022708 (2009).

[4] A.M.P. Mendez, D.M. Mitnik, and J.E. Miraglia. Depurated inversion method for orbital-specific exchange potentials. Int. J. Quantum Chem. 24 ,116 (2016).

[5] A.M.P. Mendez, D.M. Mitnik, and J.E. Miraglia. Local Effective Hartree–Fock Potentials Obtained by the Depurated Inversion Method, 76. (2018).

[6] Ionization probabilities of Ne, Ar, Kr, and Xe by proton impact for different initial states and impact energies. Nucl. Instr. Meth. Phys. Res. B 407 (2017) 236-243.

[7] J. E. Miraglia. Shell-to-shell ionization cross sections of antiprotons, H^{+}, He^{+2}, Be^{+4}, C^{+6} and O^{+8} on H, C, N, O, P, and S atoms To be published Archive 2019.

[8] Y. Iriki, Y. Kikuchi, M. Imai, and A. Itoh Phys. Rev. A **84** 052719 (2011).

[9] M. A. Rahman and E. Krishnakumar, Electron ionization of DNA bases, J. Chem. Phys. **144**, 161102 (2016).

[10] P. Mozejko and L. Sanche, Cross section calculations for electron scattering from DNA and RNA bases. Radiat Environ. Biophys **42**, 201 (2003).

[11] H. Q. Tan, Z. Mi, and A. A. Bettiol, Simple and universal model for electron-impact ionization of complex biomolecules, Phys. Rev. E 97, 032403 (2018)

[12] A. Itoh, Y. Iriki, M. Imai, C. Champion, and R. D. Rivarola, Cross sections for ionization of uracil by MeV-energy-proton impact, Phys. Rev. A **88**, 052711 (2013).

[13] A. N. Agnihotri, S. Kasthurirangan, S. Nandi, A. Kumar, M. E. Galassi, R. D. Rivarola, O. Fojón, C. Champion, J. Hanssen, H. Lekadir, P. F. Weck, and L. C. Tribedi. Ionization of uracil in collisions with highly charged carbon and oxygen ions of energy 100 keV to 78 MeV. Phys. Rev. A 85, 032711 (2012).

[14] A N Agnihotri, S Kasthurirangan, S Nandi, A Kumar, C Champion,, H Lekadir, J Hanssen, P FWeck, M E Galassi, R D Rivarola, O Fojon and L C Tribedi, Absolute total ionization cross sections of uracil ($C_4H_4N_2O_2$) in collisions with MeV energy highly charged carbon, oxygen and fluorine ions J. Phys. B **46**, 185201 (2013).

[15] C Champion, M E Galassi, O Fojón, H Lekadir, J Hanssen, R D Rivarola, P F Weck, A N Agnihotri, S Nandi, and L C Tribedi. Ionization of RNA-uracil by highly charged carbon ions. J. Phys.: Conf. Ser. **373**, 012004 (2012).

[16] W. Wolff, H. Luna, L. Sigaud, A. C. Tavares, and E. C. Montenegro Absolute total and partial dissociative cross sections of pyrimidine at electron and proton intermediate impact velocities J. Chem. Phys. **140**, 064309 (2014).

[17] M. U. Bug, W. Y. Baek, H. Rabus, C. Villagrasa, S. Meylan, A. B. Rosenfeld, An electron-impact cross section data set (10 eV–1 keV) of DNA constituents based on consistent experimental data: A requisite for Monte Carlo simulations, Rad. Phys. Chem. **130** 459–479 (2017).

[18] M. Wang, B. Rudek, D. Bennett, P. de Vera, M. Bug, T. Buhr, W. Y. Baek, G. Hilgers, H. Rabus, Cross sections for ionization of tetrahydrofuran by protons at energies between 300 and 3000 keV Phys. Rev. A **93**, 052711 (2016).

[19] W. Wolff, B. Rudek, L. A. da Silva, G. Hilgers, E. C. Montenegro, M. G. P. Homem, Absolute ionization and dissociation cross sections of tetrahydrofuran: Fragmentation–ion production mechanisms J. Chem. Phys. **151**, 064304 (2019).

[20] M. Fuss, A. Muoz, J. C. Oller, F. Blanco, D. Almeida, P. Limo-Vieira, T. P. D. Do, M. J. Brunger, G. Garca, Electron-scattering cross sections

for collisions with tetrahydrofuran from 50 to 5000 eV Phys. Rev. A **80**, 052709 (2009).

[21] D. J. Lynch, L. H. Toburen, and W. E. Wilson, Electron emission from methane, ammonia, monomethylamine, and dimethylamine by 0.25 to 2.0 MeV protons J. Chem. Phys. **64**, 2616 (1976).

[22] M.E. Rudd, Y.-K. Kim, D.H. Madison, J.W. Gallagher, Electron production in proton collisions: total cross sections, Review of Modern Physics, **57**, 965–994 (1985).

[23] H. Luna, A. L. F. de Barros, J. A. Wyer, S. W. J. Scully, J. Lecointre, P. M. Y. Garcia, G. M. Sigaud, A. C. F. Santos, V. Senthil, M. B. Shah, C. J. Latimer, and E. C. Montenegro, Water-molecule dissociation by proton and hydrogen impact, Phys. Rev. A **75** 042711 (2007).

[24] W. E. Wilson and L. H. Toburen. Electron emission from proton – hydrocarbon-molecule collisions at 0.3–2.0 MeV. Phys. Rev. A 11, 1303 (1975).

[25] D. J. Lynch, L. H. Toburen, and W. E. Wilson. Electron emission from methane, ammonia, monomethylamine, and dimethylamine by 0.25 to 2.0 MeV protons. J. Chem. Phys. 64, 2616 (1976).

[26] Multiscale approach to the physics of radiation damage with ions. E. Surdutovich and A. V. Solov'yov, arXiv:1312.0897v, (2013)

[27] P. de Vera1, I. Abril, R. Garcia-Molina and A.V.Solov'yov, Ionization of biomolecular targets by ion impact: input data for radiobiological applications. Journal of Physics: Conference Series 438 (2013) 012015

[28] Jung-Goo Lee, Ho Young Jeong, and Hosull Lee, Charges of Large Molecules Using Reassociation of Fragments. Bull. Korean Chem. Soc.24 2003, 369 .

[29] A. K. Rappe, A. K.and W. A. Goddard III,. J. Phys. Chem. **95 (**1991) 3358.

[30] A. D. Becke, J. Chem. Phys. 98, 5648-5652 (1993)

[31] P. J. Stephens, F. J. Devlin, C. F. Chabalowski, M. J. Frisch, J. Phys. Chem. 98, 11623-11627 (1994)

[32] S.M. Pimblott and J. A. LaVerne, Radiation Physics and Chemistry 76, 1244-1247 (2007)

[33] M. E. Rudd, Y.-K. Kim,, D. H. Madison and T. J. Gay. Electron production in proton collisions with atoms and molecules: energy distributions. Rev. Mod. Phys. **64**, 44-490 (1992).

[34] E. Clementi, C. Roetti, At. Data Nucl. Data Tables 14, 177–478 (1974).